Progress in the Evaluation and Validation of n+^{56,57}Fe Cross Sections

A. Trkov[1,*], *R.* Capote[2], *D.* Bernard[3], *R.* Beyer[4], *Y.* Danon[5], *A.* Daskalakis[5], *A.* Junghans[4], *M.* Kostal[6], *P.* Leconte[3], *M.* Schulc[6], and *S.* Simakov[7]

[1]Jožef Stefan Institute, Jamova 39, 1000 Ljubljana, Slovenia
[2]NAPC–Nuclear Data Section, International Atomic Energy Agency, PO Box 100, A-1400 Vienna, Austria
[3]Commisariat a l'Energie Atomique, Cadarache, DEN/DER 13108 Saint-Paul-Lez-Durance, France
[4]Helmholtz-Zentrum Dresden-Rossendorf, Bautzner Landstr. 400, 01328 Dresden, Germany
[5]Gaertner LINAC Center, Rensselaer Polytechnic Institute, Troy, NY 12180, United States
[6]Research Center Rez Ltd, 250 68, Husinec-Rez 130, Czech Republic
[7]Karlsruhe Institute of Technology, Hermann-von-Helmholtz-Platz 1 76344 Eggenstein-Leopoldshafen, Germany

Abstract. There has been a continued effort since 2019 within the IAEA INDEN collaboration to improve the evaluation of neutron induced reactions on iron isotopes. The reason for the 30% underestimation of the neutron leakage spectrum from a thick iron sphere was found primarily to be due to the overestimation of the inelastic cross sections in the ^{56}Fe evaluated data file produced within the CIELO project of the OECD/NEA Data Bank. The over-estimation of the neutron flux between the resonances near 300 keV was traced to neglecting the fluctuating nature of the total cross section of ^{57}Fe in the fast neutron energy range, since the evaluated resolved resonance range of ^{57}Fe extended only up to 190 keV. The added $1/v$ background in the "iron window" below 28 keV is in excellent agreement with the independently evaluated one in the JENDL-5.0 library that included the direct capture component in the evaluation. Performance of the updated ^{56,57}Fe evaluations was tested on a set of criticality benchmarks from the ICSBEP Handbook, including the dependence on reflector thickness and on new deep penetration shielding benchmark using a ^{252}Cf(sf) neutron source undertaken at Rez, Czech Republic. Neutron leakage for 43 MeV incident neutrons was also validated.

1 Introduction

Iron is an extremely important structural and shielding material that appears in many nuclear applications usually as a major component of stainles steel. Nuclear reaction data of iron have been addressed within the Subgroup-40 (CIELO) of the OECD/NEA Data Bank [1]. The resulting evaluated data files from the BNL/IAEA collaboration for the iron isotopes [2] were included in the ENDF/B-VIII.0 library [3] and performed well in criticality benchmarks. Unfortunately, inadequate performance of the ^{56}Fe evaluation was discovered for shielding benchmarks by Simakov [4] just before the release of the ENDF/B-VIII.0 library: the leakage spectra from very thick iron shells with a ^{252}Cf(sf) source in the centre were significantly under-predicted in the energy range 1-8 MeV (see Fig.32 of Ref. [2]). A similar under-prediction of about 30% for 14 MeV neutron source was found for neutron leakage energies from 1 to 4 MeV (see Fig.35 of Ref. [2])

The CIELO project is formally terminated [1, 5]. The International Nuclear Data Evaluation Network (INDEN) is a follow-up activity coordinated by the International Atomic Energy Agency (IAEA) to connect the evaluators in Member States to collaborate in the nuclear data evaluation efforts. Within this framework additional analysis of the iron nuclear data was performed which showed that the root cause of the problem was the inelastic cross section of ^{56}Fe, which seemed to be too high. In the CIELO evaluation the evaluated inelastic cross section was based on the Negret experiment at JRC, Geel [6], and the elastic cross section was calculated from the difference of the inelastic to the total cross section. CIELO derived elastic cross sections were in contradiction with the new measurement of the elastic cross sections by Pirovano [7] at JRC Geel. A compromise was made by reducing the inelastic cross sections and compensating the difference with the elastic cross sections such that both remained within their respective uncertainty bands and unitarity with the total cross section was preserved. However, new Beyer data [8] support Negret values in that energy region. Korzh older measurements [9] are also in agreement with Negret data. Additional studies are needed to clarify the values of the inelastic cross section below 2 MeV.

Jansky was reporting over-prediction of the neutron flux in the so-called "iron windows" between the resonances in spectra leaking through thick iron spheres with a ^{252}Cf(sf) source in the centre [10]. The effect was particularly strong around 300 keV. Trials by increasing the elastic cross section in the resonance minima were proven wrong by Beyer et al. [11] in a transmission measurement on a thick (90 mm) iron target. The root cause was iden-

*e-mail: andrej.trkov@ijs.si

© The Authors, published by EDP Sciences. This is an open access article distributed under the terms of the Creative Commons Attribution License 4.0 (https://creativecommons.org/licenses/by/4.0/).

tified to be the total cross sections of ^{57}Fe, which did not take into account the highly fluctuating nature of the cross sections above 190 keV. Largest fluctuations up to 12 barn amplitude were very different from the smoothly evaluated values of about 4 barn. These fluctuations in a minor isotope become important precisely at the minima of the elastic cross section in ^{56}Fe.

There was also a question of the thermal capture cross section. R. Firestone [12] published the results from prompt-gamma activation analysis, which suggested lowering of the thermal capture cross section by 7%. Validation measurements at CEA within the MAESTRO project [13] at the MINERVE reactor did not support such a decrease (see discussion at p.31 of Ref. [14]). The same validation showed that JEFF-3.1.1 evaluation was essentially correct, so the recommended value of the thermal capture cross section for ^{56}Fe of 2.577 barns was adopted. This value is also in agreement with latest Firestone evaluation based on historic sets of pile oscillation measurements [15].

The resulting evaluated data files were extensively tested. The benchmarking exercise illustrates how integral benchmarks can be used to discriminate between discrepant differential data to produce evaluated data files that perform well in situations that are critical for the safe operation of nuclear installations.

The evaluation methodology is briefly described in Section 2. Some details of the nuclear model calculations are summarized in Section 2.2. Specific adjustments to the cross sections are described in Section 2.3. Performance on benchmarks is described in Section 3, discussing separately the performance in criticality benchmarks in Subsection 3.1 and shielding benchmarks in Subsection 3.2. The conclusions are given in Section 4.

2 Evaluation methodology

Due to the observed large scale total cross-section fluctuations up to 4 MeV of incident neutron energy in ^{56}Fe and the inability of the optical model to properly describe the average total cross section in that energy region, a decision was made to use experimental data for the evaluation [2], it is a non-model evaluation from 850 keV up to 4 MeV [16].

Regarding the inelastic cross section in the ^{56}Fe evaluation, the key point is that we trust the total cross sections in the ENDF/B-VIII.0 evaluation. New measurements by E. Pirovano at the neutron time-of-flight facilities GELINA and nELBE support a higher elastic cross section, while capture is too small to play a role. This leads to the conclusion that the inelastic cross sections were most likely too high.

The elastic cross section was evaluated as the difference between the high-resolution total cross section by Berthold et al [17] measured on a natural Fe sample and the estimated inelastic data as shown in Fig. 2. The new elastic cross section is shown to be higher than CIELO evaluation in better agreement with Pirovano data [7] as shown in Fig.1. The elastic cross section is generally in agreement with the JEFF-3.1.1 elastic cross section as shown in the same figure.

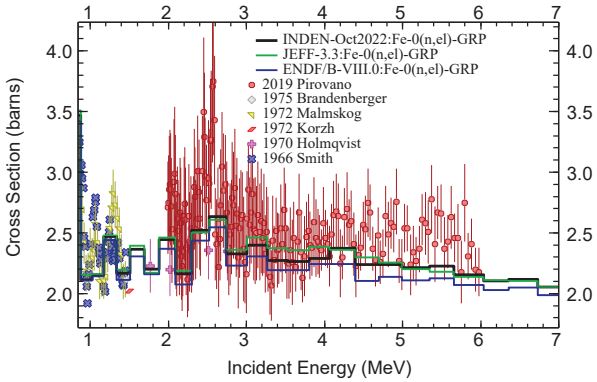

Figure 1. Comparison of the ^{nat}Fe measured elastic cross sections below 7 MeV vs ENDF/B-VIII.0, JEFF-3.1.1, and current INDEN evaluation.

The estimated inelastic cross section is close to the ENDF/B-VII.1 and JEFF-3.1.1 evaluations and shows a 10–15% reduction of evaluated data compared to Beyer [8] and Korzh [9] measurements as shown in Fig.2. The reduction is significant from 2 up to 7 MeV of incident neutron energy. Further experimental investigations of this discrepancy are planned.

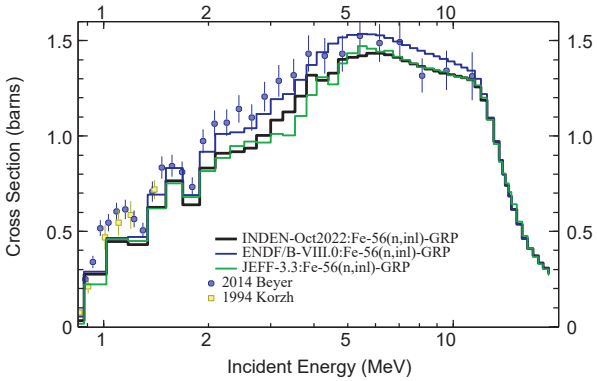

Figure 2. Comparison of low-resolution ^{56}Fe inelastic cross sections vs ENDF/B-VIII.0, JEFF-3.1.1, and current INDEN evaluation.

Legendre-polynomial fits of measured angular distributions by Kinney (above 0.85 MeV) [18] and Smith (from 2.5 to 4 MeV) [19] were directly adopted in the evaluated file (since INDEN r39 version). Perey angular distributions [20, 21] were used below 850 keV in the resolved-resonance region following a feedback provided by RPI quasi-differential iron experiment [22]. All angular-distribution Legendre polynomial fits adequately represent measured data at room temperature and are truly independent of resonance spin assignment and missing resonances. This is an advantage over angular distributions reconstructed from derived resonance parameters at zero Kelvin. The elastic angular distribution at 1.3 MeV of incident neutron energy measured by Ramirez *et al.* [23] is shown in Fig.3.

Note the significant differences between the smooth lines (point-wise data at 1.3 MeV) and the histogram derived as an incident-energy averaged over 175-energy

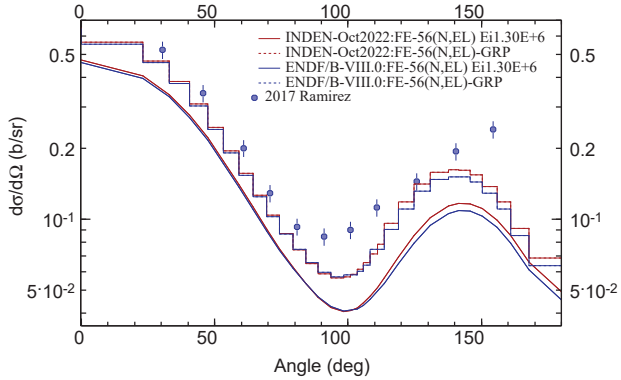

Figure 3. Comparison of the ^{nat}Fe measured elastic angular distribution at 1.3MeV of incident neutron energy vs ENDF/B-VIII.0 and current INDEN r61 evaluation.

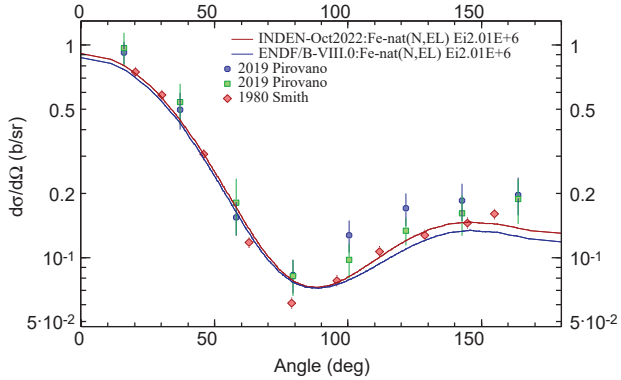

Figure 4. Comparison of the ^{nat}Fe measured elastic angular distribution at 2MeV of incident neutron energy vs ENDF/B-VIII.0 and current INDEN r61 evaluation.

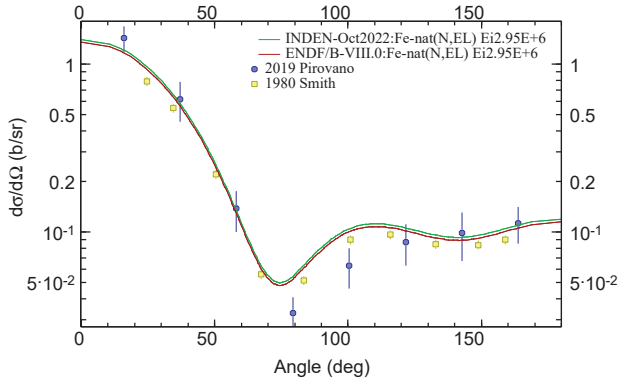

Figure 5. Comparison of the ^{nat}Fe measured elastic angular distribution at 3MeV of incident neutron energy vs ENDF/B-VIII.0 and current INDEN r61 evaluation.

groups of the evaluated angular distributions near 1.3 MeV. This difference highlights the resolution effect on the comparison of angular distributions between measured and evaluated data, Such effects are significantly reduced at higher energies. There were minor changes in the Smith data fit in the current evaluation that resulted in slightly larger anisotropy compared to the ENDF/B-VIII.0 (CIELO) evaluation as shown in Figs.4 and 5. The cross-section anisotropy changes disappear at 4 MeV of neutron incident energy as seen in Fig.6.

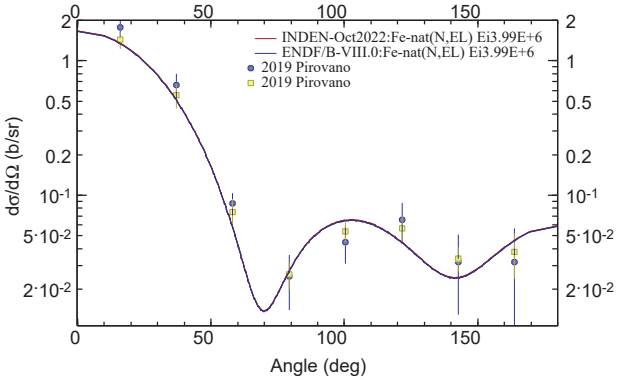

Figure 6. Comparison of the ^{nat}Fe measured elastic angular distribution at 4 MeV of incident neutron energy vs ENDF/B-VIII.0 and current INDEN r61 evaluation.

2.1 Resonance parameters

The resonance parameters of ^{56}Fe are essentially those evaluated by Perey and Perey [24] which were included in the Fröhner evaluation in the JEF-2.2 library [25]. Some typos in the original evaluation were corrected (one resonance energy was changed from 767.240 keV to 766.724 keV and the spurious resonance at 59.5 keV was deleted [2]). Fröhner's evaluation has also been adopted in subsequent JEFF libraries and in JENDL-4.0. Based on the feedback from the iron-uranium criticality benchmark ZPR-9/34 (hmi001/1 – item 7 in Table 1), which has extremely high sensitivity to capture in the region below the first s-wave resonance (1–30 keV), we effectively added a $1/v$ component to the capture cross section (see Fig.11 of Ref.[2]). This component was reduced in the current INDEN file as shown in Fig. 7. The INDEN r61 $1/v$ background in Fig. 7 was independently confirmed in the JENDL-5.0 evaluation, in which the direct capture mechanism was considered explicitly and matches very well with the current evaluation in this particular energy range.

The other cross-section change in the Fröhner evaluation was the addition of smooth background cross section to capture of up to 3.1 millibarns starting at 400 keV up to 850 keV (at the upper end of the resolved resonance range) to make the average cross sections agree with measured cross-section values at RPI (see Fig.12 of Ref.[2]). At the same time the background makes the average capture cross section below 850 keV consistent with the average capture cross section measured by McDermott *et al.* at RPI above 850 keV [27]. The added background is physically supported by direct capture calculations by Diakakis and colleagues [28] as due to the direct capture on "p" and "d" states. This higher energy background (400–850keV) remains untouched from the ENDF/B-VIII.0 evaluation.

It was already noted by Perey and Perey [24] that there are missing levels above 400 keV and they did not consider evaluated resonance parameters reliable in that energy range and suggested using average resonance parameters to describe data there. This situation imposes constraints on the use of reconstructed angular distributions from evaluated resonance parameters; non-zero angular momentum states ("p" and "d" waves) are very important

to describe the corresponding angular distributions. Unfortunately, "p" resonances and "d" resonances are often missed in the capture yield due to the increasingly higher centrifugal barrier $\tilde{l}(l+1)$ for non-zero orbital momentum states.

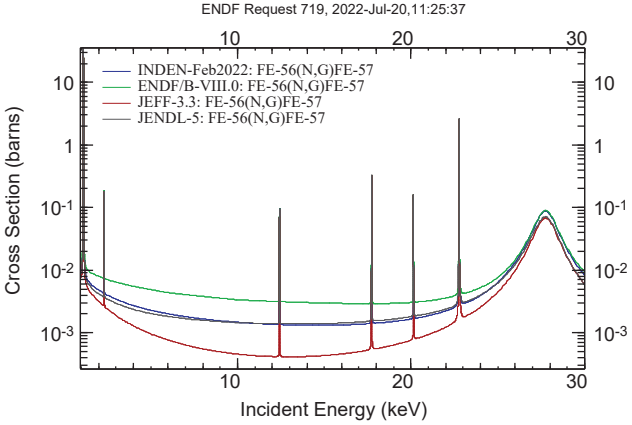

Figure 7. Comparison of the ^{56}Fe capture cross sections below 30 keV in the "iron transmission window". The current work INDEN r61 is compared with recent evaluations.

The resonance parameters of ^{57}Fe were not changed compared to the ENDF/B-VIII.0 evaluation, but the ^{57}Fe cross sections in the fast neutron range above 190 keV were modified as described in Section 2.3.

2.2 Nuclear model calculation

The details of the nuclear model calculations were already given in the original paper describing the ENDF/B-VIII.0 evaluated data library [2]. Implemented changes to the cross sections are described below.

2.3 Specific changes to cross sections

The ^{56}Fe capture cross sections above 850 keV were experimentally determined by McDermott *et al.* in 2016 using a 96% ^{56}Fe sample with a good discrimination of the gammas from the ^{56}Fe(n,n'γ) reaction [27]. Those capture cross sections were already used in the ENDF/B-VIII.0 file and were not changed for the INDEN file.

As shown through the 90 mm transmission measurement undertaken at nELBE [11] the original ENDF/B-VIII.0 (CIELO) ^{56}Fe resonance parameters which are very close to Fröhner evaluation [25] were correct; there was no need to make any changes to the cross sections in the minima of the elastic cross sections. This is shown in Fig. 8 where INDEN ^{56}Fe evaluation r39 (black solid line) is off data from 295 up to 310 keV. A similar behavior is seen at other elastic minima over the whole resolved resonance region.

Therefore, a different reason should be responsible for the observed overestimation of the neutron flux near 300 keV. It was found that the resonance range of ^{57}Fe extends only up to 190 keV, although there are significant oscillations in the total cross sections above this energy, as seen in the data of Pandey [29]. The raw Pandey data were linearized to remove some statistical fluctuations. The data

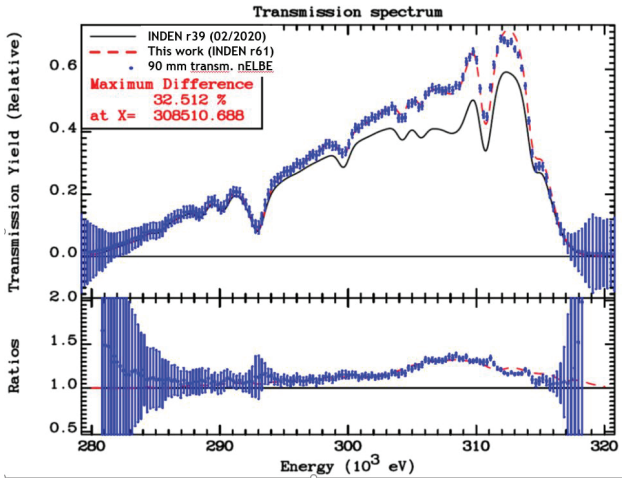

Figure 8. Simulation of the transmission measurement through a 90 mm natural iron sample at the nELBE facility, demonstrating the correctness of the updated ^{56}Fe resonance data (INDEN r61)and the ^{57}Fe fluctuating total cross sections above the resonance range (dashed red line), compared to the previous trial (black solid line – INDEN r39) with modified elastic cross sections in the minima of ^{56}Fe cross sections.

were entered in point-wise form into the ENDF file, dumping the difference between the total and the partial cross sections into the elastic cross section (see green line in Fig. 9). With these corrections the Monte Carlo simulation of the nELBE transmission experiment through a 90 mm natural iron sheet is in excellent agreement with the measured transmission, as seen for the dashed red line in Fig. 8.

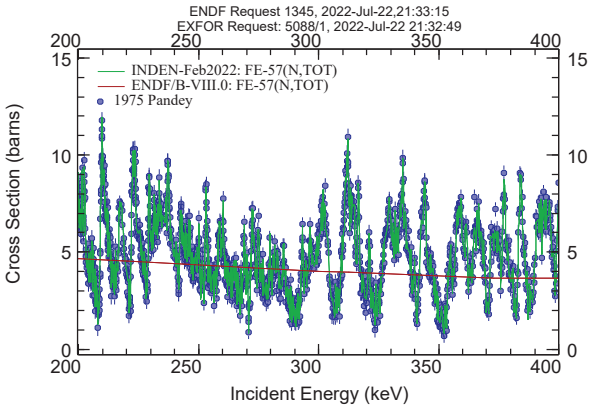

Figure 9. Comparison of the updated ^{57}Fe total cross sections (green line) with the data by Pandey (blue circles) and the original ENDF/B-VIII.0 averaged cross sections (red line).

3 Benchmarking and validation

3.1 Performance in criticality benchmarks

In the ICSBEP Handbook [30] there are many benchmarks that are sensitive to the iron cross sections, either

Table 1. Short list of ICSBEP criticality benchmark experiments sensitive to the cross sections of iron.

No.	ICSBEP Label	Short name	Common name
1	HEU-MET-FAST-013	hmf013	VNIITF-CTF-SS-13
2	HEU-MET-FAST-021	hmf021	VNIITF-CTF-SS-21
3	HEU-MET-FAST-024	hmf024	VNIITF-CTF-SS-24
4	HEU-MET-FAST-087	hmf087	VNIITF-CTF-Fe
5	HEU-MET-FAST-088	hmf088-001	FKBN-2/SS-PE-1
6	HEU-MET-FAST-088	hmf088-002	FKBN-2/SS-PE-2
7	HEU-MET-INTER-001	hmi001	ZPR-9/34
8	HEU-MET-THERM-013	hmt013-002	Planet_Fe-2
9	HEU-MET-THERM-015	hmt015	Planet_HEU/Fe/PE
10	IEU-MET-FAST-005	imf005d	VNIIEF-CTF-5
11	IEU-MET-FAST-006	imf006	VNIIEF-CTF-6
12	LEU-COMP-THERM-042	lct042-001	lct042-001
13	LEU-COMP-THERM-042	lct042-002	lct042-002
14	LEU-COMP-THERM-043	lct043-002	IPEN/MB-01
15	LEU-MET-THERM-015	lmt015-001	RB-Vinca(01)
16	MIX-COMP-FAST-001	mcf001	ZPR-6/7
17	MIX-COMP-FAST-005	mcf005s	ZPR-9/31
18	MIX-COMP-FAST-006	mcf006s	ZPPR-2
19	PU-MET-FAST-015	pmf015	BR-1-3
20	PU-MET-FAST-025	pmf025	pmf025
21	PU-MET-FAST-026	pmf026	pmf026
22	PU-MET-FAST-028	pmf028	pmf028
23	PU-MET-FAST-032	pmf032	pmf032
24	PU-MET-INTER-002	pmi002	ZPR-6/10
25	PU-MET-INTER-003	pmi003-001s	ZPR-3/58(U)
26	PU-MET-INTER-004	pmi004-001s	ZPR-4/59(Pb)
27	IEU-COMP-INTER-005	ici005	ZPR-6/6A
28	PU-MET-FAST-015	pmf015s	BR-1-3

in the form of iron blocks or in stainless steel. A selection of benchmarks was made according to the sensitivities obtained with the DICE system [31] developed at the OECD/NEA Data Bank and the availability of the computational models for the MCNP Monte Carlo transport code [32]. The selected benchmarks are listed in Table 1, giving the ICSBEP label, the short name and the common name of the benchmark.

The results are shown in Fig. 10, showing the difference between the calculated and the reference effective multiplication factor (k_{eff}) values for the ENDF/B-VIII.0 and the current INDEN r61 evaluations. From the plot it is evident that the evaluation performance of the ENDF/B-VIII.0 file was not compromised. Reactivity predicted for some of the benchmarks is closer to the benchmark reference, but there are outliers, which were not affected significantly by the changes. A biggest improvement is observed for the ZPR-6/10 benchmark (pmi002 - Case 24 in Table 1), but this improvement is mainly due to the improvements of Cr cross sections [14]. This benchmark is also sensitive to the nickel cross sections, further investigations are warranted.

Another aspect is to check the reactivity prediction of fast assemblies as a function of stainless-steel reflector thickness. In the ICSBEP Handbook there are several benchmarks with different thicknesses of stainless steel reflectors. The list ordered by reflector thickness is given in Table 2. The results on Fig. 11 with the INDEN r61 evaluation are very similar to the results with the ENDF/B-VIII.0 library. There is an small positive criticality trend with increasing reflector thickness observed for all libraries, but it is well within the benchmark uncertainty band. The JEFF-3.3 library slightly underestimates the criticality especially for small thickness reflectors. The

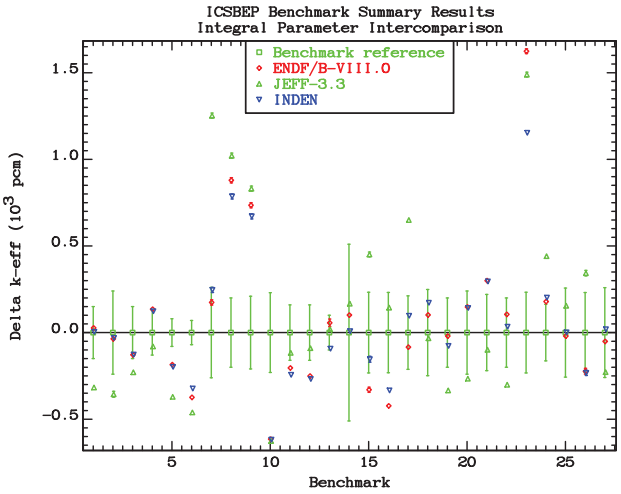

Figure 10. Comparison of the performance of ENDF/B-VIII.0, JEFF-3.3 and INDEN r61 evaluations on the selected criticality benchmarks.

gradient as a function of reflector thickness is practically the same for the three compared evaluations.

Table 2. Short list of ICSBEP criticality fast benchmarks with different thicknesses of stainless steel reflectors.

ICSBEP Label	Short name	Common name	Reflector thickness [cm]
HEU-MET-FAST-084	hmf084-019	Comet-Fe	1.27
PU-MET-FAST-025	pmf025	pmf025	1.55
HEU-MET-FAST-084	hmf084-007	Comet-Fe	2.54
HEU-MET-FAST-013	hmf013	VNIITF-CTF-SS-13	3.65
PU-MET-FAST-032	pmf032	pmf032	4.49
HEU-MET-FAST-021	hmf021	VNIITF-CTF-SS-21	9.70
PU-MET-FAST-026	pmf026	pmf026	11.9
PU-MET-FAST-028	pmf028	pmf028	19.7
PU-MET-FAST-015	pmf015s	BR-1-3	28.1

3.2 Performance in shielding benchmarks

There are many deep-penetration benchmark experiments involving iron of different quality and sensitivity. From the previous experience we needed to validate both the new iron and chromium evaluations, being the nickel evaluation taken from the ENDF/B-VIII.0 library. The most recent experiment using a well-validated neutron spectrometer was performed at Řež, CZ [33]. The experiment measured the neutron leakage spectrum from a 50x50x50cm^3 stainless steel cube with a ^{252}Cf(sf) source located inside. Comparison was made between the spectra calculated with different libraries and the measured spectrum for energies from 1 MeV up to 12 MeV. The best results of all participating libraries were obtained with the INDEN data, thus validating the current evaluation for deep penetration problems and energies above 1 MeV. This benchmark is particularly sensitive to elastic and inelastic cross sections and angular distributions, Note that a 15% underestimation of the neutron leakage using the Fe-56 CIELO evaluation adopted in ENDF/B-VIII.0 library is clearly seen in Fig.12 in the whole energy range. The JEFF-3.3 evaluation over-

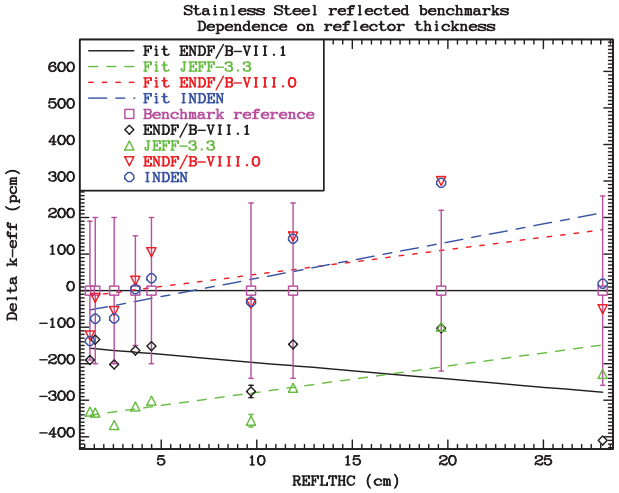

Figure 11. Comparison of reactivity prediction between ENDF/B-VIII.0, JEFF-3.3 and INDEN r61 evaluations as a function of stainless-steel reflector thickness.

estimates the measured leakage from 2 up to 4 MeV; and JENDL-4 overestimates the measured data around 5 MeV.

There are very few benchmarks to test the performance of evaluated data files on deep penetration problems above 20 MeV. One of the very few is the TIARA benchmark performed in Japan with a neutron source obtained by bombarding a lithium target with a proton beam. Leakage spectra were measured for neutrons with nominal energies of 43 MeV and 68 MeV. Spectra for incident neutrons of 43 MeV leaking from a 100 cm thick slab of iron are shown on Fig. 13. The results with older libraries like ENDF/B-VII.1 are poor. The INDEN results are almost equal to ENDF/B-VIII.0, which is reasonable since no changes were done to the evaluation at high energies. The results obtained with INDEN and ENDF/B-VIII.0 libraries are comparable to those with iron data taken from the JENDL-5.0 library.

4 Conclusions

Benchmark testing of the updated evaluated data files of iron showed significant improvement in performance. The previously observed serious deficiency of the iron CIELO evaluation of under-predicting the fast-neutron leakage spectra from thick iron shells with a ^{252}Cf(sf) source was solved. The very long-standing issue of 30% overestimation of the neutron leakage around 300 keV was also eliminated by modifying ^{57}Fe cross sections to follow Pandey experimental data above the resolved resonance region. Neutron leakage benchmark experiments with a D-T source also showed an improvement. In the TIARA benchmark involving 43 MeV incident neutrons the new evaluation performed much better than the ENDF/B-VII.1 and JEFF-3.3 libraries and comparably to the JENDL-5.0 library. At the same time, the good CIELO evaluation performance in criticality benchmarks was not compromised. The newly recommended evaluated nuclear data files are available from the International Atomic Energy Agency web page https://nds.iaea.org/INDEN/ of the INDEN project.

Acknowledgements

The IAEA is grateful to all participating laboratories for their assistance in the collaborative INDEN network and for supporting the IAEA meetings and activities. Work described in this paper would not have been possible without contributions from the IAEA Member States. R.C. acknowledges the important contributions to this work made by V. Zerkin by improving his online plotting package. Special thanks to Luiz Leal for his independent evaluations, and to the JEFF working group to study iron evaluations for inspiration and challenges.

References

[1] M.B. Chadwick *et al.*, "CIELO Collaboration Summary Results: International Evaluations of Neutron Reactions on Uranium, Plutonium, Iron, Oxygen and Hydrogen", Nucl. Data Sheets **148** (2018), 189–213.

[2] M. Herman *et al.*, "Evaluation of Neutron Reactions on Iron Isotopes for CIELO and ENDF/B-VIII.0", Nucl. Data Sheets **148** (2018) 214–253.

[3] D.A. Brown, M.B. Chadwick, R. Capote *et al*, "ENDF/B-VIII.0: The 8th Major Release of the Nuclear Reaction Data Library with CIELO-project Cross Sections, New Standards and Thermal Scattering Data", Nucl. Data Sh. **148** (2018), 1–142.

[4] S. Simakov and U. Fischer, "Validation of the latest JEFF and ENDF Evaluations by Iron Spheres with 14 MeV pulsed and ^{252}Cf sources", **JEF/DOC-1851**, NEA Nuclear Data Week, Apr 2017, Paris.

[5] M.Fleming, M.B.Chadwick, D.Brown, R.Capote, Z.Ge, M.W.Herman, A. Ignatyuk, T.Ivanova, O.Iwamoto, A.Koning, A.Plompen, A.Trkov *et al*, "Results of the Collaborative International Evaluated Library Organisation (CIELO) Project", EPJ Web of Conf. **239**, 15003 (2020).

[6] A. Negret *et al.*, "Cross-section measurements for the ^{56}Fe(n,xnγ) reactions", Phys. Rev. **C90**, 034602 (2014).

[7] E. Pirovano *et al.*, "Cross section and neutron angular distribution measurements of neutron scattering on natural iron", Phys. Rev. **C99**, 024601 (2019).

[8] R. Beyer, R. Schwengner, R. Hannaske, A.R. Junghans, R. Massarczyk, M. Anders, D. Bemmerer, A. Ferrari, A. Hartmann, T. Kögler, M. Röder, K. Schmidt, and A. Wagner, "Inelastic scattering of fast neutrons from excited states in ^{56}Fe", Nucl. Phys. **A927**, 41-52 (2014).

[9] I.A.Korzh, V.A.Mishchenko, N.M.Pravdivy, N.T. Sklyar, D.A. Bazavov, and V.P.Lunev, Ukr. Fiz. Zhur. **39**, 785 (1994),

[10] B. Jansky *et al.*, "Iron-56, problem with the elastic cross section in neutron energy region around 300 keV and natural iron isotopes influence on the neu-

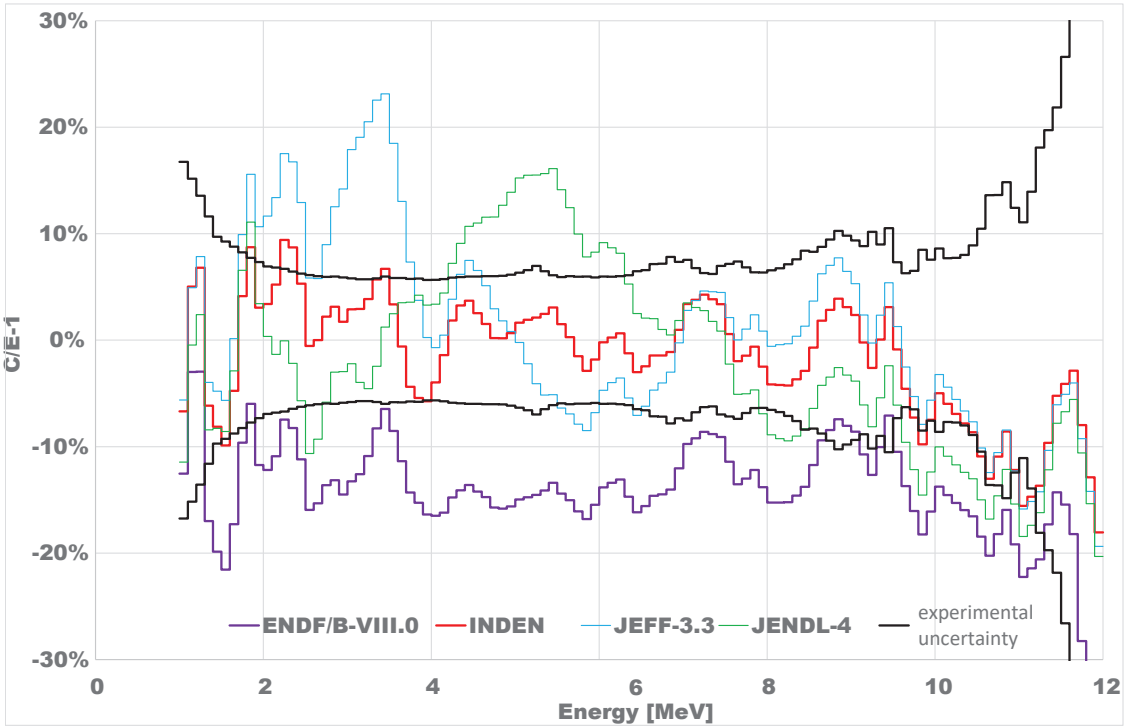

Figure 12. Comparison of the Calculated/Experimental ratio (C/E-1) of the neutron leakage spectra from a ^{252}Cf(sf) source through a 50cm side stainless steel cube.

tron transport through iron", OECD/NEA Data Bank, **JEFDOC-1919** (2018).

[11] R. Beyer, Arnd Junghans *et al.*, nELBE transmission experiment, private communication (2022), to be published.

[12] R.B. Firestone *et al.*, Thermal neutron capture cross section for ^{56}Fe(n,γ), Physical Review **C95**, 014328 (2017).

[13] P. Leconte, "Nuclear data feedback on structural, moderating and absorbing materials through the MAESTRO experimental programme in MINERVE," Tech. Rep. **JEF/DOC-1849**, Nuclear Energy Agency, OECD, Paris, France (2017)

[14] G.P.A. Nobre, M.T. Pigni, D.A. Brown, R. Capote, A. Trkov, K.H. Guber, R. Arcilla, J. Gutierrez, A. Cuadra, G. Arbanas, B. Kos, D. Bernard, and P. Leconte, "Newly Evaluated Neutron Reaction Data on Chromium Isotopes", Nucl. Data Sheets **173** 1–41 (2021).

[15] R.B. Firestone, "Renormalization of Pile Oscillator Thermal Neutron Capture Cross Section Data", International Atomic Energy Agency, Vienna, Austria, Technical report **INDC(USA)-109** (2021).

[16] R. Capote, D.L. Smith, and A. Trkov, "Nuclear data evaluation methodology including estimates of covariances", EPJ Web of Conf. **8**, 04001 (2010).

[17] K. Berthold, C. Nazareth, G. Rohr, and H. Weigman, "Total cross section of natural Fe," Private communication (1994).

[18] W.E. Kinney and J.W.McConnell, "High Resolution Neutron Scattering Experiments at ORELA", Int. Conf. on Interaction of Neutrons with Nuclei, Lowell 1976, p.1319 (1976), USA.

[19] A. Smith and P. Guenther, "Scattering of MeV Neutrons from Elemental Iron", Nucl. Sc. Eng. **73** (1980) 186–195.

[20] C.M. Perey, F.G. Perey, J.A. Harvey, N.W. Hill, and N.M.Larson, Technical report **ORNL-TM-11742**, ORNL, 1990.

[21] C.M. Perey, F.G. Perey, J.A. Harvey, N.W. Hill, and N.M.Larson, "56-Fe and 60-Ni resonance parameters", Int. Conf. on Nucl. Data for Sci. and Technol., Juelich 1991, p.41 (1991), Germany.

[22] A.M. Daskalakis, E.J. Blain, B.J. McDermott, R.M. Bahran, Y. Danon, D.P. Barry, R.C. Block, M.J. Rapp, B.E. Epping, and G. Leinweber, "Quasi-differential elastic and inelastic neutron scattering from iron in the MeV energy range", Ann. Nucl. Energy **110** 603–612 (2017).

[23] A.P.D. Ramirez, J.R. Vanhoy, S.F. Hicks, *et al.*, "Neutron scattering cross section measurements for 56Fe", Phys. Rev. **C95**, 064605 (2017).

[24] C.M. Perey and F.G. Perey, technical report **ORNL/TM-6405** (1990).

[25] F. H. Fröhner and F. Fabbri, ^{56}Fe evaluated nucelar data file, MAT2631 JEF-2.2 library, December 1989 (distr. Jan. 1992)

[26] Y. Danon, "Update on CIELO Related Nuclear Data Measurements at the Gaerttner LINAC Center at

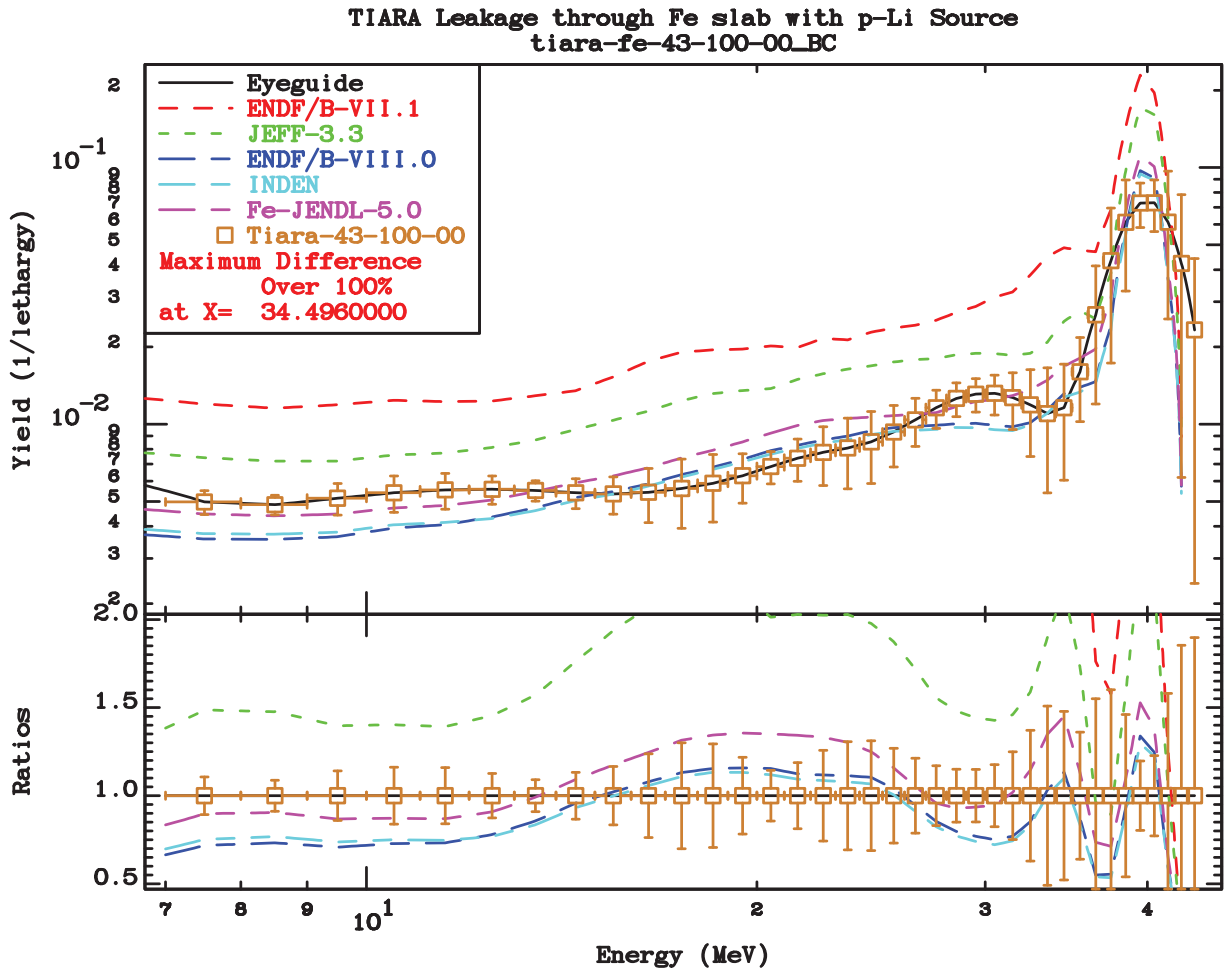

Figure 13. Comparison of the measured leakage neutron spectra yield from a 43 MeV neutron source passing through a thick iron block and calculations using different evaluated data libraries.

RPI", CIELO meeting, May 9–11, Paris, France.

[27] B. McDermott, E. Blain, N. Thompson, A. Weltz, A. Youmans, Y. Danon, D. Barry, R. Block, A. Daskalakis, B. Epping, G. Leinweber, and M. Rapp, "^{56}Fe capture cross section experiments at the RPI LINAC Center", EPJ Web of Conf. **146**, 11038 (2017).

[28] "First Results on the Direct Reaction Capture (DRC) calculations for the ^{56}Fe isotope", M. Diakaki, G. Gkatis, A. Mengoni, G. Noguere, and P. Tamagno, presented at the INDEN network meeting on Structural Materials, 13-17 December 2021, IAEA HQ, Vienna. Available online at https://www-nds.iaea.org/index-meeting-crp/CM-INDEN-strucmat-2021-12/docs/CM-INDEN-SM-2021-Diakaki.pdf.

[29] M.S. Pandey, J.A. Harvey, J.B. Garg, and W.M. Good, "Dependence of level spacing of the isotopes of iron upon parity", ORNL technical report **ORNL-5025**, p.125 (1975).

[30] ICSBEP 2020: International Handbook of Evaluated Criticality Safety Benchmark Experiments, Nuclear Energy Agency, OECD, Paris (2020). See list online at http://www.oecd-nea.org/science/wpncs/icsbep/handbook.html

[31] OECD/NEA Data Bank, Database for ICSBEP (DICE), https://www.oecd-nea.org/jcms/pl_20293/database-for-icsbep-dice

[32] MCNP—A General Monte Carlo Code for Neutron and Photon Transport, Version 5, LANL report **LA-UR-05-8617**, Los Alamos, USA (2005).

[33] M. Schulc, M. Košťál, T.Czakoj, J.Šimon, E. Novák, Z. Matěj, Comprehensive stainless steel neutron transport libraries validation, Ann. Nucl. En. **179** (2022) 109433. Benchmark detailed description and MCNP inputs available at https://nds.iaea.org/INDEN/data/ALARM-CF-steel-SHIELD-001-final.pdf